

# Late time acceleration in a slow moving galileon field

Debabrata Adak,<sup>1</sup> Amna Ali,<sup>1</sup> and Debasish Majumdar<sup>1</sup>

<sup>1</sup>*Astroparticle Physics and Cosmology Division and Centre for Astroparticle Physics, Saha Institute of Nuclear Physics, 1/AF Bidhannagar, Kolkata 700 064, India*

In this paper, we examine the cosmological viability of a slow moving galileon field in a potential. The Lagrangian  $\mathcal{L} = -\frac{1}{2}g^{\mu\nu}\pi_{;\mu}\pi_{;\nu} + \frac{G^{\mu\nu}}{2M^2}\pi_{;\mu}\pi_{;\nu}$  respects the galileon symmetry in curved space time. We carry out detailed investigations of the underlying dynamics of this Lagrangian with Einstein-Hilbert term and a potential. We demonstrate that the model can give rise to a viable ghost free late time acceleration of universe. Furthermore we study the cosmological perturbation of the model and see that the model gives different BBN constraints at early times. We also carry out the observational analysis of the model and use observational data from growth, Type Ia Supernovae (SNIa), Baryon Acoustic Oscillations (BAO) and Cosmic Microwave Background (CMB) to constrain the parameters of the theory.

## I. INTRODUCTION

From cosmological observations [1–4] it is evident that our universe is currently undergoing an accelerated expansion. The theoretical understanding of the nature of cosmic repulsion is a challenge for the cosmologist and the particle physicist today. A variety of approaches have been studied to address the problem, still till date there is no definite clue for it. According to the standard approach, the late time acceleration can be accounted for by supplementing the energy momentum tensor by an exotic fluid component with large negative pressure dubbed *dark energy* [5–12], which constitutes of about three fourth of total cosmic budget of the universe [13]. The simplest candidate of dark energy which is consistent with the observations is provided by cosmological constant  $\Lambda$ . However, there are various serious theoretical problems associated to it namely, the *fine tuning* and the *coincidence* problem.

An interesting alternative to cosmological constant is provided by the scalar fields. The cosmological dynamics of a variety of scalar field models has been studied in the literature [7]. Though these models do not address the cosmological constant problem, they can give late time cosmic acceleration and can also provide a viable cosmological dynamics at early epochs. Scalar field models with generic features like the trackers are capable of alleviating the fine tuning and coincidence problems. At present, these scalar field models are absolutely consistent with the observations but at the same time, a large number of these models are also permitted. One must therefore rely on future data which should allow to narrow down the class of permissible scalar field dark energy models.

Another interesting approach employed to explain the late time acceleration of the universe is to modify the gravity at large scale (infra-red modification of gravity). It is well known that gravity gets quantum mechanically corrected at small scales which at present is beyond our observational reach, therefore it might be possible that gravity also suffers modifications at large scales, where it is never tested directly. The modified gravity models

are either phenomenological [14] or are motivated by the higher dimensions [15]. However, any large scale modification of gravity should be capable of being distinguished from cosmological constant, should be free from ghost and tachyon instabilities and should not conflict with the local physics. A large number of modified gravity models have been investigated, among which is the galileon gravity [15]. It is motivated by the decoupling limit of the Dvali-Gabadadze-Porrati (DGP) model [16]. Galileon theories are subclass of the scalar-tensor theories involving only up to second order derivatives, which was originally found by Hordenski [19]. The Lagrangian of the galileon field  $\pi$  respects the shift or the galileon symmetry in flat space time  $\pi \rightarrow \pi + a + b_\mu x^\mu$ , where  $a$  and  $b_\mu$  are a constant and a constant vector respectively. Due to this symmetry, the equations of motion for the field contain only second derivatives. The galileon modified gravity can give rise to late time acceleration and is free from negative energy instabilities [17]. Galileon field in a potential is also studied and is shown to give a viable cosmological dynamics [18].

Recently the galileon symmetry was subsequently extended to the curved space time by the authors of [20], and was shown that the Lagrangian  $\mathcal{L} = -\frac{1}{2}g^{\mu\nu}\pi_{;\mu}\pi_{;\nu} + \frac{G^{\mu\nu}}{2M^2}\pi_{;\mu}\pi_{;\nu}$  respects this symmetry in curved space time. The sign of the terms in  $\mathcal{L}$  are chosen in such a way that, the effective propagator of  $\pi$  is never ghost-like and hence are stable. By adding the standard Einstein-Hilbert term to  $\mathcal{L}$ , and a non trivial potential for  $\pi$ , one gets a simple though rich gravitational theory, with some nice properties. In particular, in the flat space time limit and in the regimes in which the analogue of the strong energy condition is violated, the field  $\pi$  moves slower than in the cousin canonical theory. For this reason,  $\pi$  is dubbed as the “Slotheon”.

In this paper we investigate the cosmological dynamics of a model based upon slotheon gravity, set up the autonomous system and discuss the existence and stability of fixed points. We study the accelerating solution and the observational constraints on the model parameters using, growth, supernovae, BAO and CMB data. We also study the metric perturbations and investigate

the growth history of the model.

## II. BACKGROUND

In slotheon theories, the large scale modification of gravity arises due to self interaction of a scalar field  $\pi$ , which moves in a potential  $V$  and couples with matter and metric. In what follows, we shall consider the slotheon action of the form,

$$S = \int d^4x \sqrt{-g} \left[ \frac{1}{2} \left( M_{\text{pl}}^2 R - \left( g^{\mu\nu} - \frac{G^{\mu\nu}}{M^2} \right) \pi_{;\mu} \pi_{;\nu} \right) - V(\pi) \right] + \mathcal{S}_m \left[ \psi_m; e^{2\beta\pi/M_{\text{pl}}} g_{\mu\nu} \right], \quad (1)$$

where  $M_{\text{pl}}^2 = \frac{1}{8\pi G}$  is the reduced Planck mass,  $M$  is a energy scale,  $R$  is the Ricci Scalar,  $\psi_m$  is the matter field which couples to  $\pi$  and  $\beta$  is dimensionless coupling constant. Variation of this action gives the following equations of motion

$$M_{\text{pl}}^2 G_{\mu\nu} = T_{\mu\nu}^{(m)} + T_{\mu\nu}^{(r)} + T_{\mu\nu}^{(\pi)}, \quad (2)$$

$$\square\pi + \frac{1}{M^2} \left[ \frac{R}{2} \square\pi - R^{\mu\nu} \pi_{;\mu\nu} \right] - V'(\pi) = -\frac{\beta}{M_{\text{pl}}} T^{(m)}, \quad (3)$$

where  $T_{\mu\nu}^{(m)}, T_{\mu\nu}^{(r)}, T_{\mu\nu}^{(\pi)}$  corresponds to the energy momentum tensor of dust like particles, radiation and field respectively, and

$$T_{\mu\nu}^{(\pi)} = \pi_{;\mu} \pi_{;\nu} - \frac{1}{2} g_{\mu\nu} (\nabla\pi)^2 - g_{\mu\nu} V(\pi) + \frac{1}{M^2} \left[ \frac{1}{2} \pi_{;\mu} \pi_{;\nu} R - 2\pi_{;\alpha} \pi_{(\mu} R_{\nu)}^{\alpha} + \frac{1}{2} \pi_{;\alpha} \pi^{;\alpha} G_{\mu\nu} - \pi^{;\alpha} \pi^{;\beta} R_{\mu\alpha\nu\beta} - \pi_{;\alpha\mu} \pi_{;\nu}^{\alpha} + \pi_{;\mu\nu} \pi_{;\alpha}^{\alpha} + \frac{1}{2} g_{\mu\nu} [\pi_{;\alpha\beta} \pi^{;\alpha\beta} - (\pi_{;\alpha}^{\alpha})^2 + 2\pi_{;\alpha} \pi_{;\beta} R^{\alpha\beta}] \right], \quad (4)$$

where  $'$  denotes the derivative wrt  $\pi$ . It has been shown that, for  $V(\pi) > 0$ , the time derivative of the  $\pi$  field is smaller than that of a canonical scalar field with the same energy density. Therefore the  $\pi$  field is slower than a canonical scalar field [20, 21]. Though due to the presence of potential the action is not  $\pi$ -parity invariant, yet it is free from Ostrogradsky ghost problem. Also the slowing of the field  $\pi$  is solely due to gravitational interaction. In a spatially flat FLRW background, the equations of motion take the form

$$3M_{\text{pl}}^2 H^2 = \rho_m + \rho_r + \frac{\dot{\pi}^2}{2} + \frac{9H^2 \dot{\pi}^2}{2M^2} + V(\pi), \quad (5)$$

$$M_{\text{pl}}^2 (2\dot{H} + 3H^2) = -\frac{\rho_r}{3} - \frac{\dot{\pi}^2}{2} + V(\pi) + \frac{\dot{\pi}^2}{2M^2} (2\dot{H} + 3H^2) + \frac{2H\dot{\pi}\ddot{\pi}}{M^2}, \quad (6)$$

$$-\frac{\beta}{M_{\text{pl}}} \rho_m = \ddot{\pi} + 3H\dot{\pi} + \frac{3H^2}{M^2} \left( \ddot{\pi} + 3H\dot{\pi} + \frac{2\dot{H}\dot{\pi}}{H} \right) + V'(\pi). \quad (7)$$

The equation for the conservation of energy, derived from the previous equations are

$$\dot{\rho}_m + 3H\rho_m = \frac{\beta}{M_{\text{pl}}} \dot{\pi} \rho_m, \quad (8)$$

$$\dot{\rho}_r + 4H\rho_r = 0. \quad (9)$$

Let us introduce the following dimensionless variables

$$x = \frac{\dot{\pi}}{\sqrt{6}HM_{\text{pl}}}, \quad y = \frac{\sqrt{V(\pi)}}{\sqrt{3}HM_{\text{pl}}}, \quad (10)$$

$$\epsilon = \frac{H^2}{2M^2}, \quad \lambda = -M_{\text{pl}} \frac{V'(\pi)}{V(\pi)}, \quad (11)$$

required to cast the evolution equations in the form of an autonomous system

$$\frac{dx}{dN} = x \left( \frac{\ddot{\pi}}{H\dot{\pi}} - \frac{\dot{H}}{H^2} \right), \quad (12)$$

$$\frac{dy}{dN} = -y \left( \sqrt{\frac{3}{2}} \lambda x + \frac{\dot{H}}{H^2} \right), \quad (13)$$

$$\frac{d\epsilon}{dN} = 2\epsilon \frac{\dot{H}}{H^2}, \quad (14)$$

$$\frac{d\Omega_r}{dN} = -2\Omega_r \left( 2 + \frac{\dot{H}}{H^2} \right), \quad (15)$$

$$\frac{d\lambda}{dN} = \sqrt{6}x\lambda^2(1 - \Gamma), \quad (16)$$

where  $N \equiv \ln a$ ,  $\Gamma = \frac{VV_{,\pi\pi}}{V_{,\pi}^2}$  and

$$\frac{\dot{H}}{H^2} = \frac{-3x^2(1 + 24\epsilon + 108\epsilon^2) + 12\sqrt{6}x\epsilon(y^2\lambda - \beta\Omega_m)}{2(1 - 6\epsilon(x^2 - 1) + 108x^2\epsilon^2)} + \frac{(1 + 6\epsilon)(3y^2 - 3 - \Omega_r)}{2(1 - 6\epsilon(x^2 - 1) + 108x^2\epsilon^2)}, \quad (17)$$

$$\frac{\ddot{\pi}}{H\dot{\pi}} = \frac{36x^3\epsilon + \sqrt{\frac{3}{2}}(y^2\lambda - \beta\Omega_m) + 3\sqrt{6}x^2\epsilon(\beta\Omega_m - y^2\lambda)}{x + 6x\epsilon + 6x^3\epsilon(18\epsilon - 1)} - \frac{3x(1 + 6y^2\epsilon - 2\epsilon\Omega_r)}{x + 6x\epsilon + 6x^3\epsilon(18\epsilon - 1)}, \quad (18)$$

$$\Omega_m = 1 - (x^2(1 + 18\epsilon) + y^2 + \Omega_r). \quad (19)$$

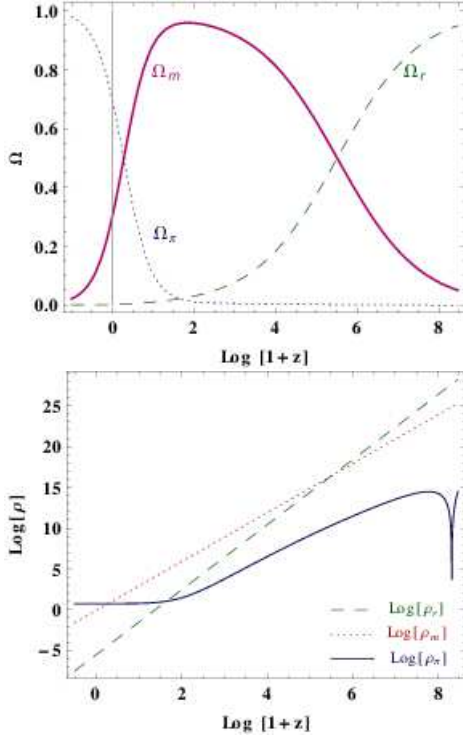


FIG. 1: (Top): Density parameters of matter( $\Omega_m$ ), radiation( $\Omega_r$ ) and field( $\Omega_\pi$ ) for potential (20) are shown here with  $\beta = 0.1$ . (Bottom): Density  $\log\left(\frac{\rho}{3M_{\text{pl}}^2 H_0^2}\right)$  for the 3 fields are shown for the same value of  $\beta$ .

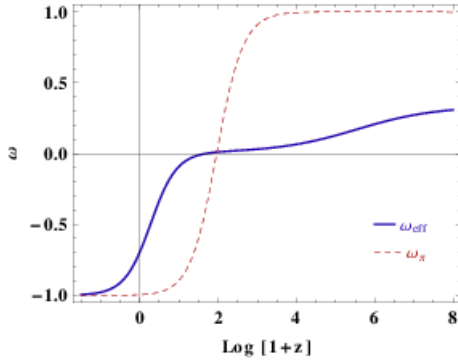


FIG. 2: The cosmic evolution of the field equation of state  $w_\pi$  and the total effective equation of state  $w_{\text{eff}}$  for  $\beta = 0.1$ .

In our analysis we consider the the exponential form of potential:

$$V(\pi) = V_0 e^{\frac{-\lambda\pi}{M_{\text{pl}}}}. \quad (20)$$

In this case we have,  $\Gamma = 1$  and therefore  $\lambda$  is a constant. Therefore the system reduces to the set of four autonomous equations. From the autonomous system, we notice that, when  $\epsilon = 0$ , the model is similar to the standard coupled dark-energy model [22]. The model has the same dynamical phase plane as that of coupled quintessence except one additional de-Sitter solution, for ( $\epsilon = -1/6, \lambda = 0, \Omega_r = 0, y^2 - 2x^2 = 1$ ). This solution exists only for the exponential form of potential. Numerical analysis of the autonomous system also depicts that the cosmology of the model is similar to the case of coupled quintessence. From Fig. 1 and Fig. 2, it is evident that, the influence of the field coupling to  $G^{\mu\nu}$  disappears fast with evolution leaving behind, the coupled quintessence scenario and providing observed cosmic acceleration at late times. The plots show tracker behavior of the field. The coupling constant  $\beta$  controls the matter phase. The parameters of the model can be fixed conveniently to produce a viable late time cosmology. We notice, that the successive sequence of radiation, matter and dark energy epochs are obtained in this model.

### III. COSMOLOGICAL PERTURBATION

In this section, we analyse the cosmological perturbation of slotheon scalar field in Newtonian gauge. The scalar perturbed metric is given by,

$$ds^2 = -(1 + 2\Psi)dt^2 + a(t)^2(1 - 2\Phi)\gamma_{ij}dx^i dx^j. \quad (21)$$

The equation for linear matter perturbation in the sub-horizon approximation is given by,

$$\ddot{\delta}_m + (2H + \frac{\beta}{M_{\text{pl}}}\dot{\phi})\dot{\delta}_m - 4\pi G_{\text{eff}}\rho_m\delta_m = 0, \quad (22)$$

where,

$$G_{\text{eff}} = G \left[ 1 + \frac{2\beta^2(1 - 6x^2\epsilon)^2 + 2x\epsilon(9x + 4\sqrt{6}(\frac{\ddot{\pi}}{H\dot{\pi}})\beta) - 12x^2\epsilon^2(-9 - 6\frac{\dot{H}}{H^2} - 4(\frac{\ddot{\pi}}{H\dot{\pi}})^2 + 3x^2 + 4\sqrt{6}(2 + \frac{\ddot{\pi}}{H\dot{\pi}})x\beta)}{1 + 2\epsilon(3 + 2\frac{\dot{H}}{H^2} - 6x^2) + 12x^2\epsilon^2(3x^2 + 8\frac{\ddot{\pi}}{H\dot{\pi}} - 4\frac{\dot{H}}{H^2} - 2) + 72x^4\epsilon^3(2\frac{\dot{H}}{H^2} - 8\frac{\ddot{\pi}}{H\dot{\pi}} - 9)} - \frac{72x^4\epsilon^3(-9 + 2\frac{\dot{H}}{H^2} - 8\frac{\ddot{\pi}}{H\dot{\pi}})}{1 + 2\epsilon(3 + 2\frac{\dot{H}}{H^2} - 6x^2) + 12x^2\epsilon^2(3x^2 + 8\frac{\ddot{\pi}}{H\dot{\pi}} - 4\frac{\dot{H}}{H^2} - 2) + 72x^4\epsilon^3(2\frac{\dot{H}}{H^2} - 8\frac{\ddot{\pi}}{H\dot{\pi}} - 9)} \right], \quad (23)$$

$\delta_m$  is the gauge invariant density contrast given by  $\delta_m = \frac{\delta\rho_m}{\rho_m} + 3Hv$ ,  $v$  being the peculiar velocity of fluid.

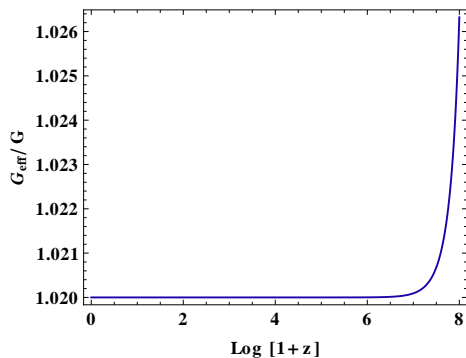


FIG. 3: Evolution of  $\frac{G_{\text{eff}}}{G}$  with  $\beta = 0.1$ .

We show the evolution of  $G_{\text{eff}}$  as a function of redshift, in Fig. 3. It is evident from the figure that, because of large gravitational strength in the past, we have  $G_{\text{eff}}$  different to General Relativity at large redshifts, whereas  $G_{\text{eff}} = G(1 + 2\beta^2) > G$  in the de Sitter phase. Thus the model reduces to coupled quintessence scenario at large scales thereby giving rise to strong cosmological constraints on  $\beta$  as we shall see in the observational analysis of the model.

#### IV. DATA ANALYSIS

This is the era of precision cosmology. Astrophysical observations can provide precise data to constrain the models of dark energy. In this work we use growth, Type Ia Supernova (SNIa), Baryon Acoustic Oscillation (BAO) and Cosmic Microwave Background (CMB) data.

We have used the growth data from the references [23]. The growth factor  $f$  is defined as:

$$f = \frac{d \ln \delta_m}{d \ln a}. \quad (24)$$

One can express the Eq.(22) in terms of the growth factor as,

$$\frac{df}{dN} + f^2 + f \left( \frac{1}{2} - \frac{3}{2}w_{\text{eff}} + \beta \frac{\dot{\pi}}{HM_{\text{pl}}} \right) - \frac{3}{2} \frac{G_{\text{eff}}}{G} \Omega_m = 0. \quad (25)$$

In Fig. 4, we show the evolution of the growth factor  $f$  for the exponential potential. In this case, the deviation from  $\Lambda$ CDM model is not significant. We also notice that  $f < 1$  for all redshift which means growth is in accordance with the Einstein-de-Sitter model. This goes well with the prediction of Dark Energy scenario.

We define

$$\chi^2 = \chi_{\text{Growth}}^2 + \chi_{\text{SN}}^2 + \chi_{\text{BAO}}^2 + \chi_{\text{CMB}}^2. \quad (26)$$

$\chi_{\text{Growth}}^2$  is defined as,

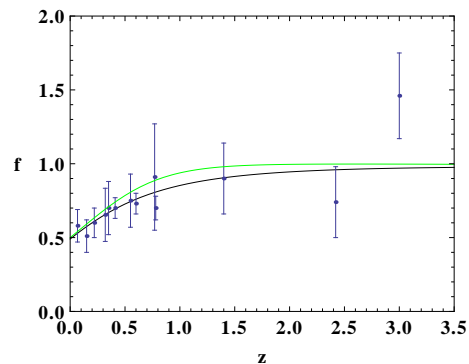


FIG. 4: Evolution of the growth factor  $f$  for the potential studied. The integration is done from  $\Omega_m \approx 0.90$  with  $\beta = 0.01$ . The green line corresponds to  $\Lambda$ CDM model.

$$\chi_{\text{Growth}}^2(\theta) = \sum_i \frac{f_{\text{obs}}(z_i) - f_{\text{th}}(z_i, \theta)}{\sigma_f(z_i)}, \quad (27)$$

where,  $f_{\text{obs}}$  is the observational growth data,  $f_{\text{th}}$  is the theoretically calculated value of growth factor of the model from the Eq.(24),  $\theta$  is the model parameter and  $\sigma_f$  is the  $1\sigma$  error. For the Supernova type Ia data, we use the latest UNION2.1 compilation [24] which contains 580 data points. The data is available in the form of distance modulus  $\mu$  with the redshift  $z$ . The distance modulus  $\mu$  is defined as,

$$\mu = m - M = 5 \log D_L + \mu_0, \quad (28)$$

where  $m$  and  $M$  are the apparent and absolute magnitudes of the Supernovae respectively,  $D_L$  is the luminosity distance defined as

$$D_L(z) = (1+z) \int_0^z \frac{H_0 dz'}{H(z')}, \quad (29)$$

and  $\mu_0 = 5 \log \left( \frac{H_0^{-1}}{M_{\text{pc}}} \right) + 25$  is a nuisance parameter which should be marginalized. The corresponding  $\chi^2$  is defined as,

$$\chi_{\text{SN}}^2(\mu_0, \theta) = \sum_{i=1}^{580} \frac{(\mu_{\text{th}}(z_i, \mu_0, \theta) - \mu_{\text{obs}}(z_i))^2}{\sigma_\mu(z_i)^2}, \quad (30)$$

where,  $\mu_{\text{obs}}$  is the observational distance modulus,  $\mu_{\text{th}}$  is the theoretical distance modulus of the model and  $\sigma_\mu$  is the error in the distance modulus. Marginalizing the nuisance parameter  $\mu_0$  as [25] we obtain,

$$\chi_{\text{SN}}^2(\theta) = A - \frac{B^2}{C}. \quad (31)$$

Where,

$$A(\theta) = \sum_{i=1}^{580} \frac{(\mu_{th}(z_i, \mu_0, \theta) - \mu_{obs}(z_i))^2}{\sigma_\mu(z_i)^2}, \quad (32)$$

$$B(\theta) = \sum_{i=1}^{580} \frac{\mu_{th}(z_i, \mu_0, \theta) - \mu_{obs}(z_i)}{\sigma_\mu(z_i)^2}, \quad (33)$$

$$C(\theta) = \sum_{i=1}^{580} \frac{1}{\sigma_\mu(z_i)^2}. \quad (34)$$

We have used the BAO data of  $\frac{d_A(z_*)}{D_V(Z_{BAO})}$  [26–29], where  $z_*$  is the decoupling time  $z_* \approx 1091$ ,  $d_A$  is the comoving angular-diameter distance given by  $d_A(z) = \int_0^z \frac{dz'}{H(z')}$  and  $D_V(z) = \left(d_A(z)^2 \frac{z}{H(z)}\right)^{\frac{1}{3}}$ . Data required for this analysis is depicted in table I. We calculate  $\chi_{BAO}^2$

as described in Ref. [30], where it is defined as,

$$\chi_{BAO}^2 = X_{BAO}^T C_{BAO}^{-1} X_{BAO}. \quad (35)$$

Where,

$$X_{BAO} = \begin{pmatrix} \frac{d_A(z_*)}{D_V(0.106)} - 30.95 \\ \frac{d_A(z_*)}{D_V(0.2)} - 17.55 \\ \frac{d_A(z_*)}{D_V(0.35)} - 10.11 \\ \frac{d_A(z_*)}{D_V(0.44)} - 8.44 \\ \frac{d_A(z_*)}{D_V(0.6)} - 6.69 \\ \frac{d_A(z_*)}{D_V(0.73)} - 5.45 \end{pmatrix} \quad (36)$$

and the inverse covariance matrix,

$$C^{-1} = \begin{pmatrix} 0.48435 & -0.101383 & -0.164945 & -0.0305703 & -0.097874 & -0.106738 \\ -0.101383 & 3.2882 & -2.45497 & -0.0787898 & -0.252254 & -0.2751 \\ -0.164945 & -2.45499 & 9.55916 & -0.128187 & -0.410404 & -0.447574 \\ -0.0305703 & -0.0787898 & -0.128187 & 2.78728 & -2.75632 & 1.16437 \\ -0.097874 & -0.252254 & -0.410404 & -2.75632 & 14.9245 & -7.32441 \\ -0.106738 & -0.2751 & -0.447574 & 1.16437 & -7.32441 & 14.5022 \end{pmatrix}. \quad (37)$$

Finally for the constraints from CMB we have used the CMB shift parameter  $R = H_0 \sqrt{\Omega_{m0}} \int_0^{1089} \frac{dz'}{H(z')}$ , where  $\Omega_{m0}$  is the present density parameter of matter and  $H_0$  is the present Hubble parameter. The  $\chi_{CMB}^2$  is defined as,

$$\chi_{CMB}^2(\theta) = \frac{(R(\theta) - R_0)^2}{\sigma^2} \quad (38)$$

Where,  $R_0 = 1.725 \pm 0.018$  [31].

We have carried out this analysis on two model parameters  $\beta$  and  $\Omega_{m0}$ . To examine the constraints on  $\beta$  and  $\Omega_{m0}$  we varied  $\beta$  from  $-0.3$  to  $1$  and  $\Omega_{m0}$  from  $0.2$  to  $0.35$ . Fig. 5 shows the  $1\sigma$  and  $2\sigma$  contours in the  $(\beta, \Omega_{m0})$  parameter space. The total  $\chi^2$  minimum is at  $\beta \sim 0.014$  and  $\Omega_{m0} \sim 0.287$ . We use these best fit values of the model parameters to plot the growth index  $\gamma$  in Fig. 6 with the  $1\sigma$  and  $2\sigma$  errors. We notice that at late time, when  $w > -1$ , the evolution is consistent with Dark Energy models [32]. But the value of  $\gamma$  of the model at all redshift is large compared to that of  $\Lambda$ CDM. This is a unique characteristic of this model as it is different in case of  $f(R)$ -gravity models [33] or scalar-tensor theories [34] where  $\gamma < 0.55$ .

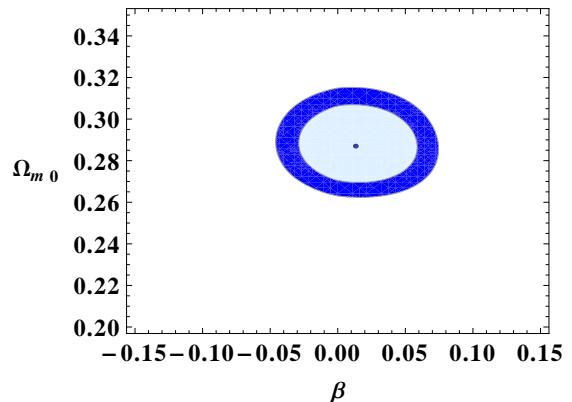


FIG. 5: The  $1\sigma$ (light) and  $2\sigma$  (dark) likelihood contours in the  $(\Omega_{m0}, \beta)$  phase plane for total  $\chi_{Growth+SN+BAO+CMB}^2$ . The point in the centre depicts the best fit values of  $(\Omega_{m0}, \beta)$ .

## V. CONCLUSION

In this paper we have investigated the slotheon gravity model with a potential. The slotheon gravity in general respects the galileon symmetry in curved space time. Here the field  $\pi$  has less kinetic energy than the canonical scalar field. Though adding a potential breaks the

$z_{BAO}$	0.106	0.2	0.35	0.44	0.6	0.73
$\frac{d_A(z_*)}{D_V(z_{BAO})}$	$30.95 \pm 1.46$	$17.55 \pm 0.60$	$10.11 \pm 0.37$	$8.44 \pm 0.67$	$6.69 \pm 0.33$	$5.45 \pm 0.31$

TABLE I: Values of  $\frac{d_A(z_*)}{D_V(z_{BAO})}$  for different values of  $z_{BAO}$ .

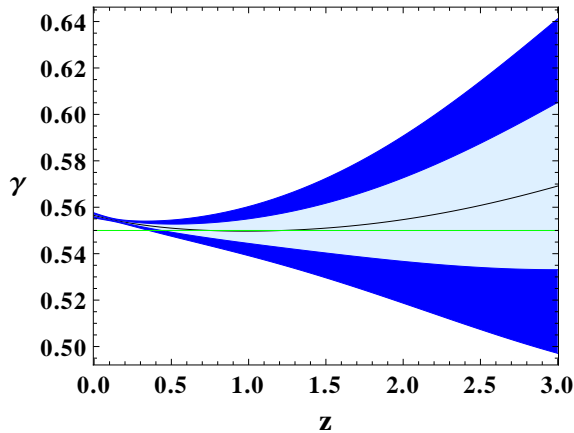


FIG. 6: The  $1\sigma$  (light) and  $2\sigma$  (dark) of the growth index. The central line is the growth index for the best fit values of the model parameters  $\beta$  and  $\Omega_{m0}$ . The green line corresponds to  $\Lambda$ CDM model.

symmetry, but it serves an important role in obtaining a viable cosmology. We have studied the model taking the exponential form of the potential. We have demonstrated that the model gives an accelerating universe at late times. We found that the cosmology of the model is similar to the case of coupled quintessence at late times

thereby giving current cosmic acceleration.

We have investigated the perturbation of this model. The deviation of the growth factor compared to  $\Lambda$ CDM model is negligible. The growth is in accordance with the Einstein-de-Sitter model. In the case of pure coupled quintessence, we have  $G_{\text{eff}} = G(1 + 2\beta^2)$  which requires the coupling to be small in order to respect the BBN constraint. On the other hand, it is interesting to note that in the model under consideration,  $G_{\text{eff}}$  is large in the higher redshift than in General Relativity which certainly gives different BBN constraints.

We have also imposed observational constraints on the model parameters using the data from growth, SNIa, BAO, and CMB observations. Constructing the corresponding contour plots we deduced that  $\beta$  is constrained by the data to small range of values  $-0.05 < \beta < 0.08$  and the density of matter today is constrained around the concordance values. The model under consideration shows larger value of growth index for all redshift compared to  $\Lambda$ CDM.

## VI. ACKNOWLEDGEMENTS

A.A thanks Radouane Gannouji for useful discussions. D.A thanks Atanu Kumar for discussions on the cosmological perturbation theory.

- 
- [1] S. Perlmutter *et al.* [Supernova Cosmology Project Collaboration], *Astrophys. J.* **517** (1999) 565 [arXiv:9812133[astro-ph]].
- [2] A. G. Riess *et al.* [Supernova Search Team Collaboration], *Astron. J.* **116** (1998) 1009 [arXiv:9805201[astro-ph]].
- [3] D. N. Spergel *et al.* [WMAP Collaboration], *Astrophys. J. Suppl.* **170** (2007) 377 [arXiv:0603449[astro-ph]].
- [4] U. Seljak *et al.* [SDSS Collaboration], *Phys. Rev. D* **71** (2005) 103515 [arXiv:0407372[astro-ph]].
- [5] V. Sahni and A. A. Starobinsky, *Int. J. Mod. Phys. D* **9**, 373 (2000).
- [6] V. Sahni and A. Starobinsky, *Int. J. Mod. Phys. D* **15**, 2105(2006)[astro-ph/0610026]; T. Padmanabhan, astro-ph/0603114; P. J. E. Peebles and B. Ratra, *Rev. Mod. Phys.* **75**, 559 (2003); L. Perivolaropoulos, astro-ph/0601014; N. Straumann, arXiv:gr-qc/0311083; J. Frieman, arXiv:0904.1832; M. Sami, *Lect. Notes Phys.* **72**, 219(2007); M. Sami, arXiv:0901.0756 .
- [7] E. J. Copeland, M. Sami and S. Tsujikawa, *Int. J. Mod. Phys., D* **15**, 1753(2006)[arXiv:0603057[hep-th]].
- [8] E. V. Linder, *Rep. Prog. Phys.* **71** (2008) 056901.
- [9] R. R. Caldwell and M. Kamionkowski, *Ann. Rev. Nucl. Part. Sci.* **59** (2009) 397 [arXiv:0903.0866 [astro-ph.CO]].
- [10] A. Silvestri and M. Trodden, *Rept. Prog. Phys.* **72** (2009) 096901 [arXiv:0904.0024 [astro-ph.CO]].
- [11] J. Frieman, M. Turner and D. Huterer, *Ann. Rev. Astron. Astrophys.* **46** (2008) 385 [arXiv:0803.0982 [astro-ph]].
- [12] M. Sami, *Curr. Sci.* **97** (2009) 887 [arXiv:0904.3445 [hep-th]].
- [13] Planck Collaboration: 2013 results, arXiv:1303.5076 [astro-ph].
- [14] S. Capozziello, *Int. J. Mod. Phys. D* **11** (2002) 483; S. Capozziello, S. Carloni and A. Troisi, *Recent Res. Dev. Astron. Astrophys.* **1** (2003) 625.
- [15] A. Nicolis, R. Rattazzi, and E. Trincherini, *Phys. Rev. D* **79** (2009) 064036; C. Deffayet, G. Esposito-Farese, and A. Vikman, *Phys. Rev. D* **79** (2009) 084003.
- [16] G. R. Dvali, G. Gabadadze and M. Porrati, *Phys. Lett. B* **485** (2000) 208 [arXiv:0005016[hep-th]].
- [17] R. Gannouji and M. Sami, *Phys. Rev. D* **82** (2010) 024011 [arXiv:1004.2808 [astro-ph]]; Amna Ali, R. Gannouji and M. Sami, *Phys. Rev. D* **82** (2010) 103015 [arXiv:1008.1588[astro-ph]].
- [18] Amna Ali, R. Gannouji, Md. Wali Hossain, M. Sami *Phys. Lett. B* **718** (2012) 10009 [arXiv:1207.3959[astro-ph]].
- [19] G. W. Hordenski, *Int. J. Theor. Phys.* **10** (1974) 363-384.

- [20] Cristiano Germani, Luca Martucci and Parvin Moyasari, arXiv:1108.1406[hep-th].
- [21] Cristiano Germani, arXiv:1207.6414[hep-th].
- [22] L. Amendola, Phys. Rev. D **62** (2000) 043511 [arXiv:9908023[astro-ph]].
- [23] E. Hawkins *et al.*, Mon. Not. Roy. Astron. Soc. **346** (2003) 78 [arXiv:astro-ph/0212375];  
E. V. Linder, arXiv:0709.1113 [astro-ph];  
L. Verde *et al.*, Mon. Not. Roy. Astron. Soc. **335** (2002) 432 [arXiv:0112161 [astro-ph]];  
C. Blake *et al.*, Mon. Not. Roy. Astron. Soc. **415** (2001) 2876 [arXiv:1104.2948];  
R. Reyes *et al.* Nature. **464** (2010) 256 [arXiv:1003.2185 [astro-ph]];  
M. Tegmark *et al.*, Phys. Rev. D **74** (2006) 123507 [arXiv:0608632 [astro-ph]];  
N. P. Ross *et al.*, arXiv:0612400 [astro-ph];  
L. Guzzo *et al.*, Nature. **451** (2008) 541;  
J. da Angela *et al.*, arXiv:0612401 [astro-ph];  
P. McDonald *et al.* [SDSS Collaboration], Astrophys. J. **635** (2005) 761 [arXiv:0407377 [astro-ph]];  
F. Beutler *et al.*, (2012), [arXiv:1204.4725];  
J. Dosset *et al.*, JCAP **1004** (2010) 022  
M. de Viel, M. G. Haehnelt and V. Springel, Mon. Not. Roy. Astron. Soc. **354** 684 (2004)
- [24] N. Suzuki *et al.* 2012 ApJ 746 85 [arXiv:1105.3470 [astro-ph]]
- [25] R. Lazkoz, S. Nesseris and L. Perivolaropoulos, JCAP **0511** (2005) 010.
- [26] W. J. Percival *et al.* [SDSS Collaboration], Mon. Not. Roy. Astron. Soc. **401** (2010) 2148, [arXiv:0907.1660[astro-ph.CO]].
- [27] F. Beutler, C. Blake, M. Colless, D. H. Jones, L. Staveley-Smith, L. Campbell, Q. Parker and W. Saunders *et al.*, Mon. Not. Roy. Astron. Soc. **416** (2011) 3017 [arXiv:1106.3366 [astro-ph.CO]].
- [28] N. Jarosik, C. L. Bennett, J. ‘Dunkley, B. Gold, M. R. Greason, M. Halpern, R. S. Hill and G. Hinshaw *et al.*, Astrophys. J. Suppl. **192** (2011) 14 [arXiv:1001.4744 [astro-ph.CO]].
- [29] C. Blake, E. Kazin *et al.*, Mon. Not. Roy. Astron. Soc. **418** (2011) 1707[arXiv:1108.2635 [astro-ph.CO]].
- [30] R. Giotri *et al.*, JCAP **1203** (2012) 027 [arXiv:1203.3213 [astro-ph]]
- [31] E. Komatsu *et al.*, ApJS **192** (2011) 18.
- [32] D. Polarski and R. Gannouji, Phys. Lett. B **660** (2008) 439 [arXiv:0710.1510 [astro-ph]].
- [33] R. Gannouji, B. Moraes and D. Polarski, JCAP **0902** (2009) 034 [arXiv:0809.3374[astro-ph]].
- [34] R. Gannouji and D. Polarski, JCAP **0805** (2008) 018 [arXiv:0802.4196[astro-ph]].